

Optically Pumped Free-Electron Laser with Electrostatic Reacceleration

Prepared by

R. HOF LAND, JR.
Aerophysics Laboratory

and

D. C. PRIDMORE-BROWN
Space Sciences Laboratory
Laboratory Operations

29 September 1989

Prepared for

SPACE SYSTEMS DIVISION
AIR FORCE SYSTEMS COMMAND
Los Angeles Air Force Base
P. O. Box 92960
Los Angeles, CA 90009-2960

Contract No. F04701-88-C-0089



Laboratory Operations

THE AEROSPACE CORPORATION

PLEASE RETURN TO:

APPROVED FOR PUBLIC RELEASE AND TECHNICAL INFORMATION CENTER
DISTRIBUTION UNLIMITED BALLISTIC MISSILE DEFENSE ORGANIZATION
7100 DEFENSE PENTAGON
WASHINGTON D.C. 20301-7100

19980309 199

U5182

Accession Number: 5182

Publication Date: Sep 29, 1989

Title: Optically Pumped Free-Electron Laser With Electrostatic Reacceleration

Personal Author: Hofland, R.; Pridmore-Brown, D.C.

Corporate Author Or Publisher: The Aerospace Corporation Laboratory Operations, El Segundo, CA
90425 Report Number: TOR-0089(4060-03)-1

Report Prepared for: Space Systems Division, Air Force Systems Command, Los Angeles Air Force Base,
P.O. Box 92960 Los Angeles, CA 90009-2960 Report Number Assigned by Contract Monitor: STARL

Comments on Document: STARLAB RRI

Descriptors, Keywords: Optical Free Electron Laser FEL Electrostatic Accelerator Reacceleration
Pumping Space Moderate Power Continuously Tunable Generator Infrared Two Stage Validation Model
Time Dependent

Pages: 17

Cataloged Date: Jul 15, 1994

Contract Number: F04701-88-C-0089

Document Type: HC

Number of Copies In Library: 000001

Record ID: 29088

Source of Document: RRI

OPTICALLY PUMPED FREE-ELECTRON LASER
WITH ELECTROSTATIC REACCELERATION

Prepared by

R. Hofland, Jr.
Aerophysics Laboratory

and

D. C. Pridmore-Brown
Space Sciences Laboratory

29 September 1989

Laboratory Operations
THE AEROSPACE CORPORATION
El Segundo, CA 90245

Prepared for

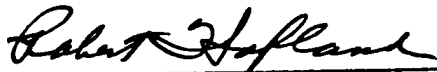
SPACE SYSTEMS DIVISION
AIR FORCE SYSTEMS COMMAND
Los Angeles Air Force Base
P.O. Box 92960
Los Angeles, CA 90009-2960

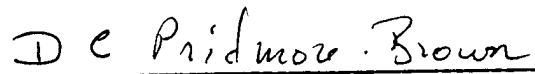
Contract No. F04701-88-C-0089

APPROVED FOR PUBLIC RELEASE;
DISTRIBUTION UNLIMITED


OPTICALLY PUMPED FREE-ELECTRON LASER
WITH ELECTROSTATIC REACCELERATION

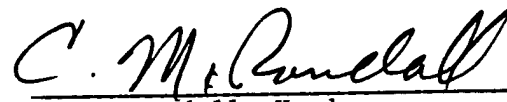
Prepared by



R. Hofland, Jr.
Aerophysics Laboratory


D. C. Pridmore-Brown
Space Sciences Laboratory

Approved by


W. P. Thompson, Director
Aerophysics Laboratory


C. M. Randall, Head
Mathematics and Analysis Department


H. R. Rugge, Director
Space Sciences Laboratory

ABSTRACT

A numerical model of a two-stage free-electron laser (FEL) was developed that considers optical pumping and time-dependent electrostatic acceleration in the laser interaction region. Analytical solutions were obtained in weak- and strong-signal limits that provide confidence in the predictions of the numerical model. The validated model predicts encouraging FEL performance when a high-current electrostatic accelerator is used as the electron source for the two-stage concept. Although the model neglects diffraction, refractive guiding, and three-dimensional and collective effects, their inclusion would not be expected to change the general conclusions reached in the present study.

ACKNOWLEDGMENT

This work was partially funded under an Aerospace Sponsored Research grant.

FIGURES

1. Phase diagram at entrance and exit of FEL interaction region
(optical pump with electrostatic reacceleration)..... 9
2. Phase diagram at entrance and exit of FEL interaction region
(optical pump with electrostatic reacceleration)..... 12
3. Electrostatic reacceleration--proof of principle experiment
(startup of FIR oscillator)..... 13
4. Second-stage oscillator performance with electrostatic
reacceleration and optical pump..... 15

OPTICALLY PUMPED FREE-ELECTRON LASER WITH ELECTROSTATIC REACCELERATION

The primary object of the present investigation is to evaluate the potential of free-electron lasers (FELs) for moderate-power continuously tunable applications in space. Specific goals include the development of theoretical models for the prediction of FEL performance, and the possible demonstration of a coherent generator that continuously spans the spectral region between 2 μm and 1 cm.

Applications for moderate-power lasers exist in short-wavelength infrared/long-wavelength infrared (SWIR/LWIR) bandpasses where high peak-power coherent sources do not exist. The continuous tunability of an FEL permits selection of any desired transmission or sensor-effects window. Important far-infrared (FIR) applications of FELs can also be identified. For example, high-power radar sources above 35 GHz do not now exist. A single-stage low-voltage FEL should provide an efficient transmitter of high-power coherent radiation spanning the wavelength range of 200 μm to 1 cm (30 GHz).

Recently, gigawatt peak powers and 45% conversion efficiencies were reported from a single-stage, tapered-undulator FEL amplifier. Amplifier experiments in high-energy linear accelerators (linacs) are being performed at several laboratories to validate present understanding of FEL injector performance, regenerative and cumulative electron-beam breakup, optical guiding and transverse mode control, energy recovery, and harmonic suppression and sideband control. Extension of these initial high-gamma experimental results to high average-power levels appears assured by the maturity of the underlying linac and electron storage-ring technologies. [Gamma in the present context refers to the relativistic factor defined by $\gamma = (1 - v^2/c^2)^{-1/2}$.] However, the development of inexpensive, low-power FELs for space applications requires an entirely different approach from the single-stage high-power configurations that are currently being studied.

For a single-stage FEL, laser output wavelength is related to wiggler magnet period λ_w by the approximate relationship $\lambda_1 = \lambda_w/2\gamma^2$. To achieve tunable single-stage operation in the SWIR and LWIR spectral regions using low-gamma beams would require orders of magnitude reduction in the period of the physical wiggler magnet (typically, 1 to 5×10^{-2} cm, or less). We propose a novel way to accomplish this goal using a two-stage FEL in which the microwave radiation from the first stage acts as the pump wave of short wavelength for the infrared second stage (Ref. 1). The output wavelength from the second stage then becomes $\lambda_2 = \lambda_1/4\gamma^2 = \lambda_w/8\gamma^4$, and short wavelengths are seen to be achievable using low-gamma beams. Inasmuch as the pitch of the magnet (laser) pump cannot be tapered in the second stage, an electrostatic field will be applied along the interaction region to achieve an efficient extraction. The field from the electrostatic reaccelerator provides power to the electron beam at roughly the same rate that coherent radiation is produced, to maintain resonance throughout the interaction. For cases where startup from spontaneous synchrotron emission is excessively long, we propose to use low-power optical injection and frequency scanning about the injected laser frequency. The validated Aerospace model, as we show, predicts encouraging performance for various applications when a high-current Van de Graaff accelerator is used as the electron source for the two-stage FEL concept.

A numerical FEL model was developed in previous studies that satisfies momentum and energy conservation in three-dimensional velocity space and includes self-consistent optical field growth and phase evolution. The effects of initial transverse electron-beam velocity and variable wiggler intensity and field pitch were also included. The model was used to study FIR amplifier extraction, oscillator transient and steady-state characteristics, saturation behavior, and power extraction for cold beams (Ref. 2). Such an FEL would be tunable over the FIR spectral region and would be of interest for high-power radar applications. The radiation from the FIR stage could also be focused into the second stage of a low-gamma FEL in order to produce tunable infrared lasing.

In the present study, major effort was expended to generalize the previously developed FEL model to include an electromagnetic (optical) pump and electrostatic reacceleration in the interaction region. Thus, it was possible to analyze the second-stage FEL problem for the first time (Refs. 3 and 4). The axial dependence of the optical wave number was also included in the numerical simulation; its inclusion enhanced electron trapping and energy transfer at low laser intensity levels, and permitted realistic simulation of the effects of e-beam energy spread on laser performance. The new formulation can easily be modified to account for space charge effects. Analytical solutions were also obtained for an optically pumped FEL with electrostatic acceleration in both the weak-signal and power-saturated cases. The predictions of the comprehensive Aerospace FEL model compare favorably with these analytic solutions in both the weak- and strong-signal limits. Performance of a two-stage FEL using an electrostatic accelerator has been analyzed with the newly developed model.

For an optically pumped FEL with electrostatic reacceleration, we take circularly polarized (electromagnetic) pump and laser fields to have only transverse components whose magnitudes are functions of the axial coordinate z . Electric and magnetic fields are written in terms of the accelerating axial electric field \vec{E}_A and the vector potential \vec{A} as

$$\vec{E} = \vec{E}_A - \partial \vec{A} / \partial t$$

$$\vec{B} = \nabla \times \vec{A}$$

where \vec{A} is the superposition of two circularly polarized fields, the laser field \vec{A}_l and the pump field \vec{A}_p , traveling in opposite directions along the interaction region. \vec{A} is given by the expressions

$$\begin{aligned} \vec{A}_l = A_l(z) [& \hat{x} \cos(\theta_l - \omega_l t + \phi_l) \\ & - \hat{y} \sin(\theta_l - \omega_l t + \phi_l)] \end{aligned}$$

$$\vec{A}_p = A_p(z) [\hat{x} \cos(\theta_p + \omega_p t + \phi_p) + \hat{y} \sin(\theta_p + \omega_p t + \phi_p)]$$

Here, $\theta_\ell = \int_0^z k_\ell(z) dz$, $\theta_p = \int_0^z k_p(z) dz$, $k = \omega/c$, and ϕ_ℓ , ϕ_p are arbitrary phase angles. Substitution of the preceding field expressions into the relativistic equations of motion governing the electron dynamics gives, after some manipulation, the following differential equations for γ and phase difference ψ :

$$\frac{d\gamma}{dt} = \frac{e}{mc} E_A - \left(\frac{e}{mc}\right)^2 \frac{\omega_\ell - \omega_p}{\gamma} A_\ell A_p \sin \psi \quad (1)$$

$$\frac{d\psi}{dt} = 2k_p c \left[1 - \frac{k_\ell(1 + \alpha^2)}{4k_p \gamma^2} \right] \quad (2)$$

where

$$\psi = \omega_p t - \omega_\ell t + \theta_\ell + \theta_p + \phi$$

$$\phi = \phi_\ell + \phi_p$$

$$\alpha^2 = (eA/mc)^2$$

and

$$A = A_\ell + A_p$$

Equation (1) is recognized as the energy conservation equation for electrons. The second term on the right-hand side of Eq. (1) arises from the fact that the pump wave gives the electrons a transverse velocity component upon which the transverse laser electric field can do work. Depending on the electrons' initial position within a radiation wavelength (i.e., the

sign of $\sin \psi$), electrons can lose or gain energy by this mechanism, resulting in optical gain or absorption. If energy is added to the electrons by the axial field E_A so that $\dot{\gamma} = 0$ on the average, then the electron transverse velocity can maintain its phase orientation relative to the transverse electric field over many pump wavelengths, resulting in electron trapping and growth of the optical field intensity (gain). The resonant particle energy follows from $\dot{\psi} = 0$ in Eq. (2), or

$$\gamma_R = \frac{1}{2}[(\omega_\ell/\omega_p)(1 + \alpha^2)]^{1/2} \quad (3)$$

The condition that $\dot{\psi}$ vanish ensures that energy extraction is a maximum from trapped electrons clustered about the resonant energy. The laser frequency is obtained from Eq. (3) as

$$\omega_\ell = 4\gamma_R^2 \omega_p (1 + \alpha^2)^{-1} \quad (4)$$

Equations (1) and (2) must be supplemented by relations for A_ℓ and A_p . Because $\omega_p \ll \omega_\ell$, one can show that $\dot{A}_p \ll \dot{A}_\ell$. The interaction between the pump wave and the electrons can, therefore, be neglected so that $A_p \approx \text{const.}$ The variation of A_ℓ follows from energy conservation as

$$I(z) = I_0 + j \left[\int_0^z E_A dz - \frac{mc^2}{e} \langle \Delta\gamma \rangle \right] \quad (5)$$

where $I(z) = (\partial A_\ell / \partial t)^2 (\mu_0 c)^{-1}$ is the intensity of the laser beam, j is the e-beam current density, and $mc^2 \langle \Delta\gamma \rangle$ is the energy change averaged over all the electrons. For highly relativistic electrons, the time derivatives d/dt can be replaced by spatial derivatives cd/dz . Then Eqs. (1), (2), and (5), together with the definition of $I(z)$, constitute a closed system of $2n + 1$ equations for n electrons. We have numerically solved these coupled nonlinear equations for one- and two-stage FEL cases of interest in the proposed space application. To test the code predictions, we first derived closed-form solutions in the small-signal and saturated limits that we now summarize.

In the small-signal limit, the variation of A_ℓ can be neglected. Then, we need only consider Eqs. (1) and (2) in the analysis. Differentiation of Eq. (2) and substitution of Eq. (1) in the resulting expression gives the governing equation

$$\frac{d^2\psi}{dt^2} = -4k_p c [(\omega_\ell - \omega_p) \left(\frac{e}{mc\gamma}\right)^2 A_\ell A_p \sin \psi - \frac{e}{mc\gamma} E_A] \quad (6)$$

We have solved Eq. (6) by perturbation methods in the small-signal limit. The expression for the overall FEL gain G with electrostatic acceleration has been derived as part of our analysis. Expressing G as $[G_0 f_0(\Omega T) - G_1 f_1(\Omega T)]$, one can show that

$$G_0 = mc \frac{2\Lambda^2 \gamma K^2}{8\Omega^3 \omega_p} \frac{j}{e} \frac{\Omega^3 T^3}{\epsilon_0 c E^2} \quad (7a)$$

$$= \left(\frac{eL}{m\gamma c}\right)^3 j \lambda_p B_p^2$$

$$f_0(\theta) = (2 - 2 \cos \theta - \theta \sin \theta) \theta^{-3} \quad (7b)$$

$$G_1 = \frac{1}{2} G_0 K V T^2 = 2k_p L \frac{e E_A L}{mc^2 \gamma} G_0 \quad (7c)$$

$$f_1(\theta) = [\theta(6 + 2 \cos \theta) - \frac{\theta^3}{3} - 8 \sin \theta] \theta^{-5} \quad (7d)$$

where $L = cT$ is the overall length of the interaction region. Retaining terms of order γ^{-2} and invoking Eq. (3), one finds that

$$\theta = \Omega T = 2k_p L (1 - \gamma_R^2 / \gamma^2) \quad (7e)$$

Numerical evaluation of Eq. (7b) shows that $f_0(\theta)$ peaks at a value of 0.135 when $\theta = 2.61$. Therefore, in the absence of an accelerating field ($G_1 = 0$), an optimum value of the gain can be achieved by injecting electrons slightly above resonance such that $(4k_p L \delta\gamma) / \gamma = 2.61$. However, in the absence of an axial field, the electrons will lose energy to the laser field and eventually $\delta\gamma$ (and the gain) will be reduced to zero. If, instead, an accelerating field of magnitude $eE_A L / mc^2 = \delta\gamma / 2$ is introduced, the electrons can be held near an optimum energy value above resonance throughout the interaction. The optimum value of E_A is

$$E_A = 1.3 mc^2 \gamma / 4k_p e L^2 \quad (8)$$

A numerical example illustrates the magnitudes of the quantities predicted by our small-signal analysis. Assume $\gamma = 4$, $B_p = 1$ kG ($I_p = 250$ MW/cm²), $L = 1.5$ m, $j = 100$ A/cm², and $\lambda_p = 0.06$ cm. Then, $\lambda_g = 9.4$ μ m, $G_0 = 81j$ (A/cm²) λ_p (cm) B_p^2 (kG) L^3 (m) $\lambda^{-3} = 25.6$, $f_0(2.6) = 0.135$, $G_1 = 1.3$, $G_0 = 33$, $f_1(2.6) = 0.01$, and $G = 3.46 - 0.33 = 3.13$. The first-order correction involving E_A is small in this case and satisfies the assumptions of the perturbation analysis. Note that a very substantial zero power gain (2%/cm) is predicted for the two-stage FEL operating at 9.4 μ m.

A computer simulation of this and other cases that consider 100 or more electrons in the small-signal limit yields results that are very close to the predictions of this analysis. For example, for the case of no accelerating field ($E_A = 0$) and with electron injection above resonance by an amount $\delta\gamma = 2.61\gamma / (4k_p L) = 1.66 \times 10^{-4}$, the simulation predicts a gain of 3.39 at an incident intensity of 200 W/cm², in close agreement with the perturbation analysis. When an accelerating field $E_A L = 173$ V is applied in accordance with Eq. (8), the simulation predicts a gain of 3.2, again in excellent agreement with the small-signal analysis. When the increase in

laser intensity with distance [Eq. (5)] is included in the simulation in a self-consistent way, the predicted gain can be higher than that given by the preceding analysis. For the preceding example, with $I_0 = 200 \text{ W/cm}^2$, the gain predicted by the self-consistent simulation is 6.7. This increase in gain is due to an increased trapping of the electrons in the ponderomotive potential well. The effect is illustrated in Fig. 1. An initial distribution of electrons is shown in Fig. 1a as a phase plot of $\gamma - \gamma_R$ vs ψ . This distribution was selected to simulate a realistic experimental situation in which the electrons are uniformly distributed in phase space, with a thermal spread of $\Delta\gamma/\gamma = 5 \times 10^{-5}$, and are injected above resonance such that $\delta\gamma = 1.66 \times 10^{-4}$. The solid line represents the separatrix, or bucket, that defines the electron trapping region where the initial intensity I_0 is 200 W/cm^2 . Figure 1b is a plot of the same electrons at the end of the interaction region where I has increased to $GI_0 = 1.26 \times 10^3 \text{ W/cm}^2$. It can be seen that many originally untrapped electrons have been captured in their transit through the interaction region.

During the course of this work, the opposite regime of large laser intensities near saturation was considered in detail. A simple analytical description illustrates the physics at saturation. The oscillator case is of major interest. Here, a fixed fraction C_{Op} of the final intensity, $I_f = I_0 + \Delta I$ at the end of the interaction region is outcoupled, and the remainder is introduced into the interaction region as a new I_0 . In this regime, we assume perfect trapping of a fraction of the electrons such that the energy lost by these electrons to the optical field is replenished by the axial electric field. We may, therefore, neglect $\langle \Delta\gamma \rangle$ in Eq. (5) for the trapped electrons and write

$$\Delta I = f j \int_0^L E_A dz \quad (9)$$

where $f = \langle \sin \psi \rangle$ is the fraction of electrons that is trapped. As the laser intensity grows with each subsequent oscillator pass, so also must

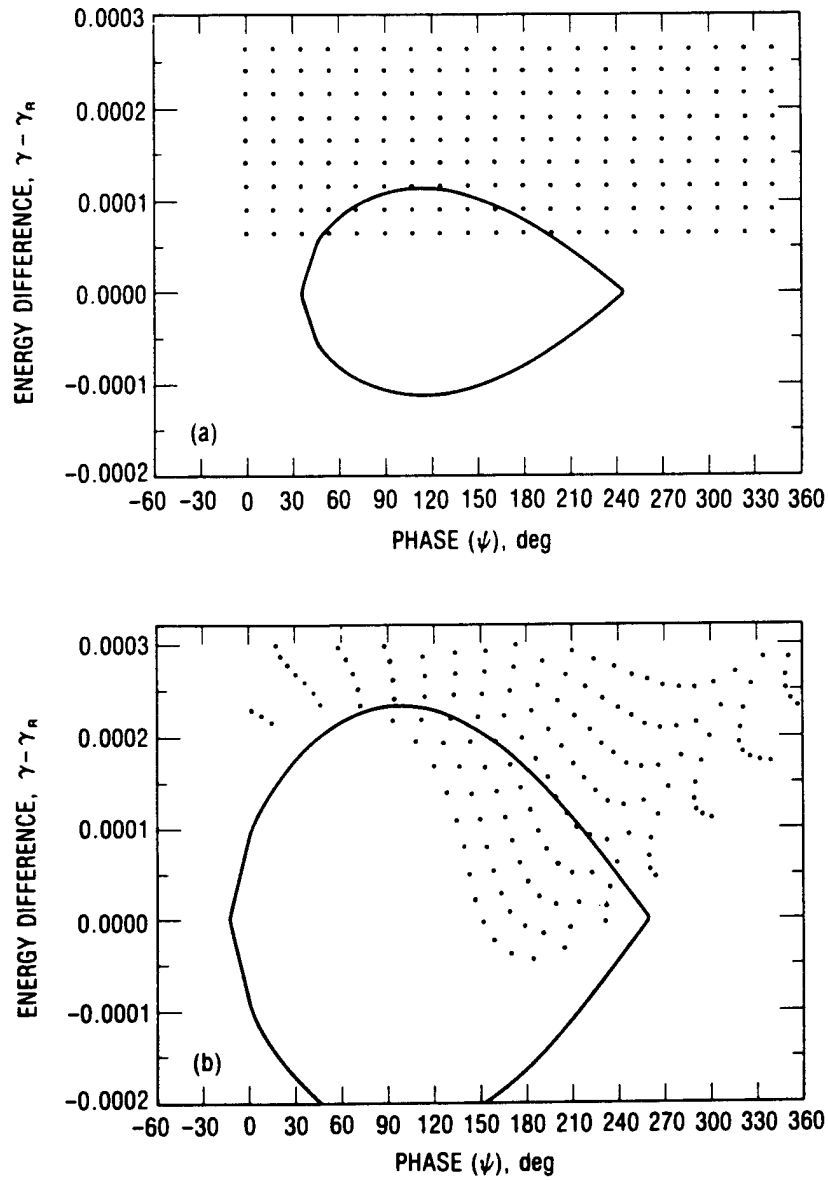


Fig. 1. Phase diagram at (a) entrance and (b) exit of FEL interaction region (optical pump with electrostatic reacceleration). For (a), $I_0 = 200 \text{ W/cm}^2$, $\gamma = 4$, $B_p = 1 \text{ kG}$, $\lambda_p = 0.06 \text{ cm}$, $j = 100 \text{ A/cm}^2$, $\Delta\gamma/\gamma = 5 \times 10^{-5}$. For (b), $I_0 = 200 \text{ W/cm}^2$, $\gamma = 4$, $B_p = 1 \text{ kG}$, $\lambda_p = 0.06 \text{ cm}$, $j = 100 \text{ A/cm}^2$, $L = 1.5 \text{ m}$, $\Delta\gamma/\gamma = 5 \times 10^{-3}$, $G = 12.6$.

the axial electric field be increased according to the relationship $E_A(t) \sim I_0^{1/2}(t)$. A more careful analysis (Ref. 4) shows that the maximum bucket size is achieved when E_A in Eq. (1) is selected such that $d\gamma/dt = 0$ at $\psi = \sin^{-1}(0.41) = 24^\circ$. Under these conditions, Eqs. (1) and (9) may be combined to give the optimum value of E_A as

$$E_A = 0.41 \frac{e}{mc} \frac{\omega_L - \omega_p}{\gamma} A_L A_p \quad (10)$$

$$\approx 0.41 \left(\frac{2\mu_0}{c} \right)^{1/2} \frac{eB_p}{m\gamma k_p} I_0^{1/2}$$

At saturation

$$I_{out} = C_{0p} I_f = \frac{C_{0p}}{1 - C_{0p}} I_0 = \Delta I \quad (11)$$

Combining Eqs. (9) through (11) yields

$$I_{out} = (0.41) \frac{2\mu_0}{c} \left[\frac{eB_p \lambda_p j L f}{m 2\pi \gamma} \right]^2 \left(\frac{1 - C_{0p}}{C_{0p}} \right) \quad (12)$$

$$= 1.1 \times 10^6 (C_{0p}^{-1} - 1) (B_p \lambda_p j L f / \gamma)^2 \quad (12a)$$

where Eq. (12a) is expressed in mks units. Comparison of Eq. (12) with the full numerical FEL simulation shows that it correctly expresses the sensitivity of saturated, optically pumped FEL performance to experimental variables for the case of time-dependent electrostatic acceleration. In our previous example, for which $B_p = 1$ kG, $\lambda_p = 600$ μm , $\gamma = 4$, $j = 100$ A/cm², $C_{0p} = 10\%$, and $L = 1.5$ m, Eqs. (11) and (12) predict saturated performance of an optically pumped FEL with electrostatic reacceleration to be $I_f = 1.11 I_0 = 5f^2$ MW/cm². In the saturated limit, gain balances loss and $G = C_{0p}/(1 - C_{0p}) = 1/9$. At intensities below saturation, gain for

trapped electrons increases monotonically with decreasing intensity to its maximum value at the small-signal limit. Results of the full numerical simulation for this case are illustrated graphically in Fig. 2, which shows phase plots at FEL intensities that are very close to saturation, for which $I_0 = 1 \text{ MW/cm}^2$ and $I_f = 1.092 \text{ MW/cm}^2$. The calculated gain of 0.092 implies that the optically pumped FEL is operating at a power level that is slightly below saturation. In Fig. 2a electrons are assumed to have an energy spread of $\Delta\gamma/\gamma = 5 \times 10^{-5}$ and are injected slightly above resonance at the beginning of the interaction. The same electrons are shown in Fig. 2b at the end of the interaction region. In contrast to the low-intensity case shown in Fig. 1b, the untrapped electrons here are seen to have moved out of the region of the figure. The fraction of electrons that is trapped is easily determined from Fig. 2b to be $f = 0.56$. The preceding approximate closed-form analysis predicts $I_f = 5f^2 \text{ MW/cm}^2 = 1.57 \text{ MW/cm}^2$ for this example, in close agreement with the full numerical simulation.

The validated model was used to investigate performance of two-stage FELs in which the current source is a high-brightness Van de Graaff accelerator. Simulation of the electrostatic concept, so crucial to the successful operation of a two-stage FEL, was carried out for a single-stage FIR FEL with our model. Selected results are shown in Fig. 3 at conditions achievable in the proposed experiment: $B_w = 2 \text{ kG}$, $\lambda_w = 2 \text{ cm}$, $\gamma = 4$, $L = 2 \text{ m}$, $\Delta\gamma/\gamma = 2 \times 10^{-3}$, and $\lambda_\rho = 0.06 \text{ cm}$. Outcoupled FIR intensity and re-accelerator potential are plotted as a function of number of resonator round trips, with beam current density as a parameter. At 100 A/cm^2 , the outcoupled intensity at $600 \mu\text{m}$ is 33 MW/cm^2 after five oscillator passes. Required reacceleration voltage is 1.2 MV , and system electrical efficiency $I_\rho / j(mc^2\gamma + V_A)$ is 10%. Note that, for the important limit, $C_{0p} = 0$, where high circulating power is desired (as in the two-stage FEL demonstration), internal fluxes of approximately 150 MW/cm^2 ($B_p \approx 0.8 \text{ kG}$) should be achievable, depending on the care with which internal cavity losses are controlled.

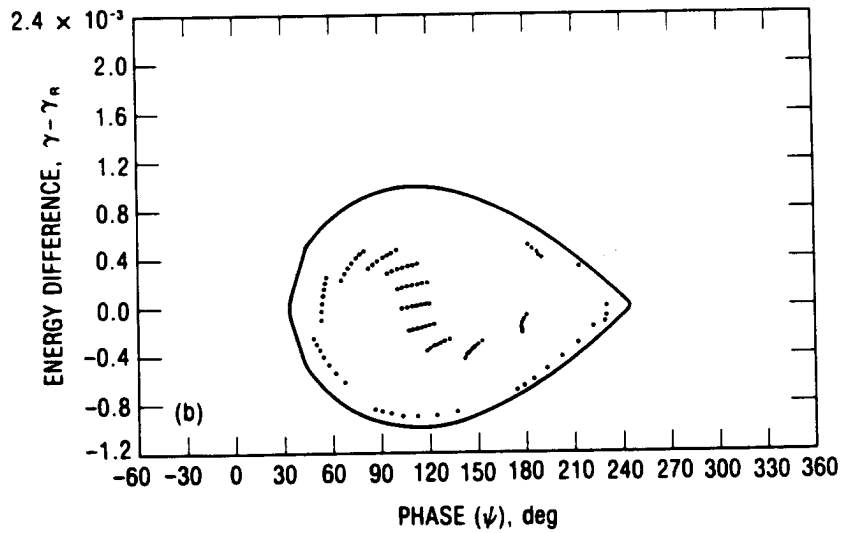
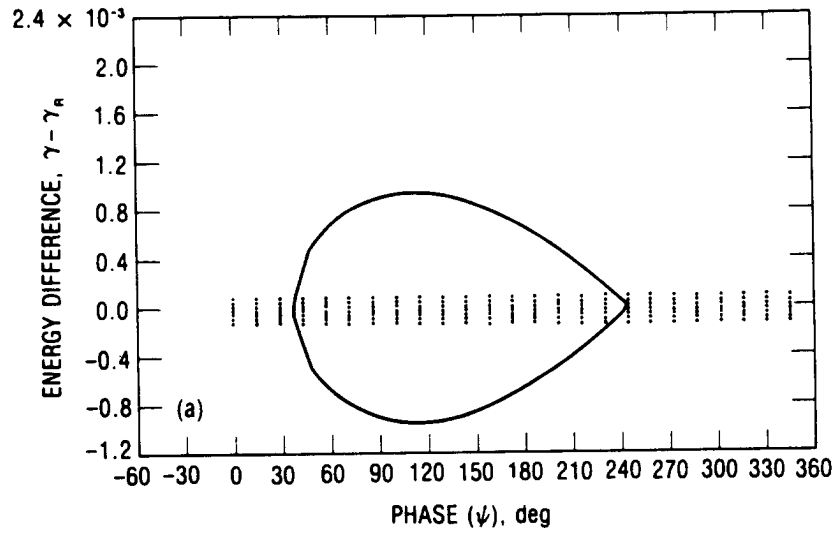


Fig. 2. Phase diagram at (a) entrance and (b) exit of FEL interaction region (optical pump with electrostatic reacceleration). For (a), $I_0 = 1 \text{ MW/cm}^2$, $\gamma = 4$, $B_p = 1 \text{ kG}$, $\lambda_p = 0.06 \text{ cm}$, $j = 100 \text{ A/cm}^2$, $\Delta\gamma/\gamma_p = 5 \times 10^{-5}$. For (b), $I_0 = 1 \text{ MW/cm}^2$, $G = 0.092$, $\gamma = 4$, $B_p = 1 \text{ kG}$, $\lambda_p = 0.06 \text{ cm}$, $j = 100 \text{ A/cm}^2$, $L = 1.5 \text{ m}$, $\Delta\gamma/\gamma_p = 5 \times 10^{-5}$.

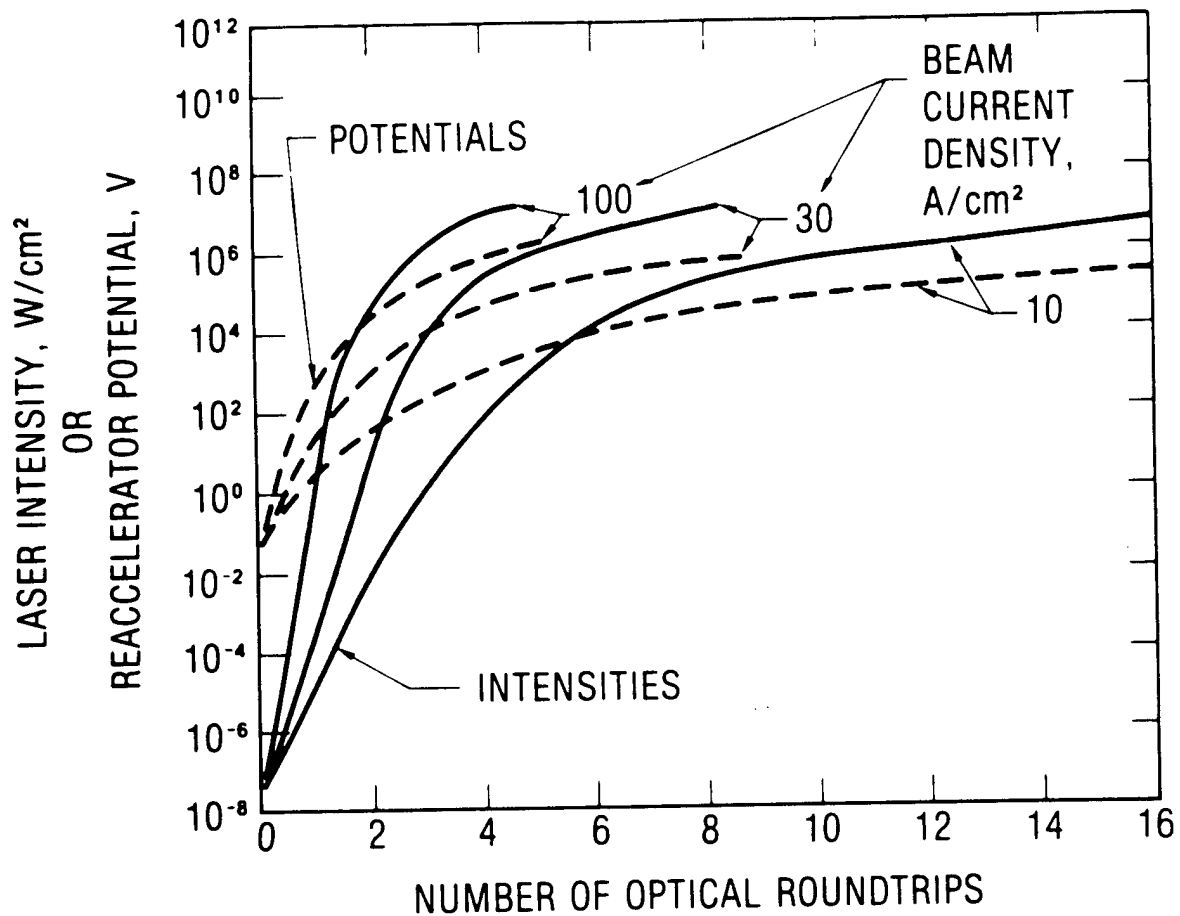


Fig. 3. Electrostatic reacceleration--proof of principle experiment (startup of FIR oscillator). $B_w = 2$ kG, $\lambda_w = 2$ cm, $\gamma = 4$, $L = 2$ m, $\Delta\gamma/\gamma = 2 \times 10^{-3}$, and $\lambda_g = 0.06$ cm.

Second-stage performance in which an optical pump and electrostatic reacceleration are used was also extensively modeled with the new FEL code. Typical performance at LWIR wavelengths ($9.4 \mu\text{m}$) is illustrated in Fig. 4, where the outcoupled laser intensity is plotted versus the number of optical round trips to saturation, beginning with optical injection at 100 W/cm^2 . (Because of low gain in the short-wavelength case, optical injection may be required if long oscillator startup times of several microseconds must be avoided.) For the calculations shown in Fig. 4, we assume a pump field of 1 kG (250 MW/cm^2) and an energy spread of $\Delta\gamma/\gamma = 4 \times 10^{-4}$. When energy spreads increase above 10^{-3} , performance falls significantly below the plotted results, emphasizing the importance of maintaining good beam quality. For the case of 100 A/cm^2 current density, the code predicts a laser output of 2 MW/cm^2 after 50 passes ($1 \mu\text{s}$); corresponding reacceleration voltage and overall electrical efficiency are seen to be 80 kV and 1.5% , respectively. (Note that, if the electrostatic field were removed, extraction efficiencies of $\lambda_p/4L \approx 0.01\%$ would be expected.) With a 20-A beam extracted from a pulsed Van de Graaff accelerator, these numerical simulations imply tunable infrared laser pulse energies of 0.6 J and average output powers of 60 W at 100 Hz repetition frequencies. Such power levels appear useful for space applications enumerated earlier in this report.

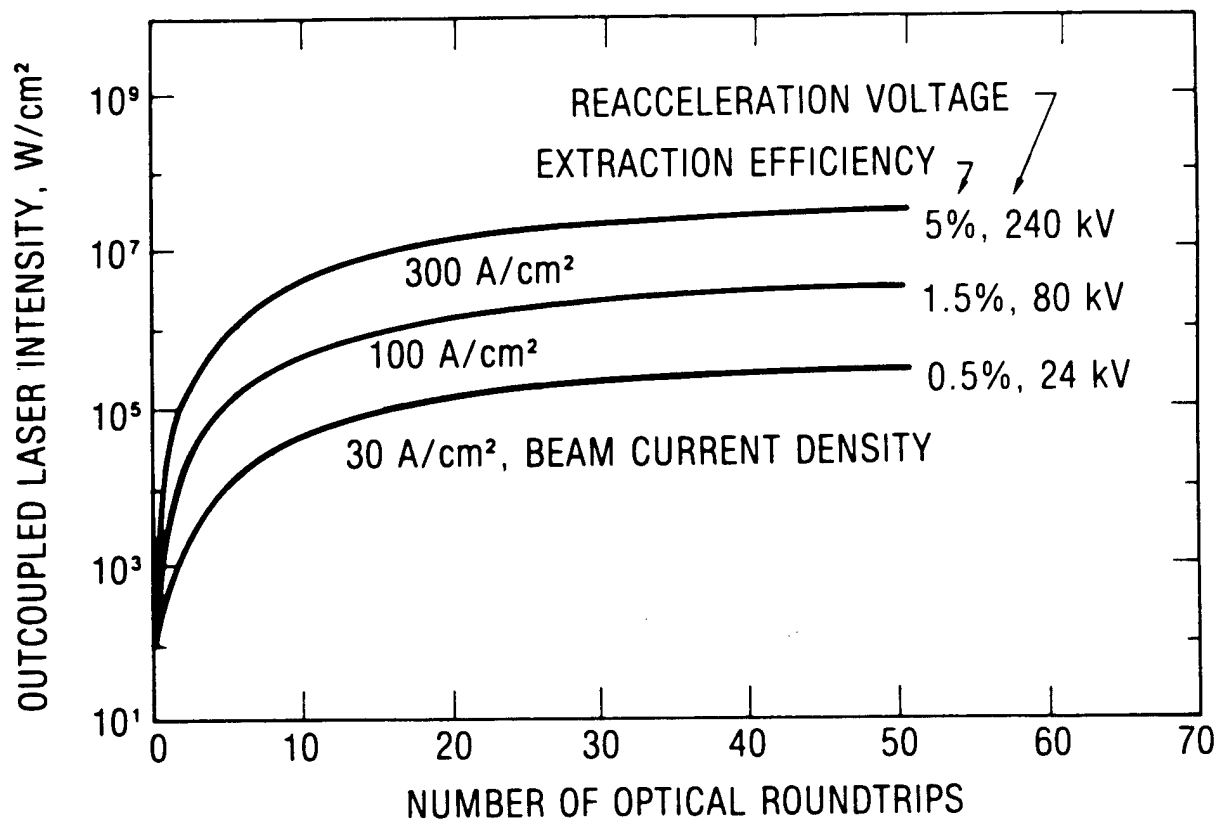


Fig. 4. Second-stage oscillator performance with electrostatic reacceleration and optical pump. $\gamma_p = 600 \mu\text{m}$, $B_p = 1 \text{ kG}$, $\gamma = 4$, $L = 2.25 \text{ m}$, $C_{Op} = 10\%$, $\Delta\gamma/\gamma = 4 \times 10^{-4}$, $\lambda_g = 9.4 \mu\text{m}$.

REFERENCES

1. L. R. Elias, Phys. Rev. Lett. 42, 977 (1979).
2. D. C. Pridmore-Brown and R. Hofland, Jr., "Low-Gamma Continuously-Tunable IR Free-Electron Laser," Advances in Laser Engineering and Applications, Vol. 247, ed. M. L. Stitch, SPIE (31 July 1980), pp. 79-84.
3. D. C. Pridmore-Brown and R. Hofland, Jr., "Two-Stage Free-Electron Laser with Electrostatic Reacceleration," Aerospace Sponsored Research Summary Report (1 December 1981), pp. 46-51.
4. H. R. Hiddlestone, S. B. Segall, and G. C. Catella, "Gain-Enhanced Free-Electron Laser with an Electromagnetic Pump Field," Free-Electron Generators of Coherent Radiation, Physics of Quantum Electronics, Vol. 9, Addison-Wesley, Reading, MA (1982), p. 849.